Journal of Applied Physics ARTICLE scitation.org/journal/jap

Adiabatically preparing quantum dot spin states in the Voigt geometry

Cite as: J. Appl. Phys. **125**, 024305 (2019); doi: 10.1063/1.5079412
Submitted: 30 October 2018 · Accepted: 18 December 2018 ·
Published Online: 10 January 2019

Emmanuel Paspalakis,[1,a)] Sophia E. Economou,[2] and Fernando Carreño[3]

AFFILIATIONS

[1]Materials Science Department, School of Natural Sciences, University of Patras, 265 04 Patras, Greece
[2]Department of Physics, Virginia Tech, Blacksburg, Virginia 24061, USA
[3]Facultad de Óptica y Optometría, Universidad Complutense de Madrid, Avenida Arcos de Jalón 118, 28037 Madrid, Spain

[a)]**Electronic mail:** paspalak@upatras.gr

ABSTRACT

We use mutually delayed and partially overlapping optical pulses, similar to those used in stimulated Raman adiabatic passage and its variations, for the coherent control of quantum dot spin states in the Voigt geometry. We consider the quantum dot system initially in an incoherent mixture of the two electron-spin states. We show that the application of regular delayed and partially overlapping pulses can lead to initialization. In addition, if initially delayed, partially overlapping, and simultaneously switched off pulses are applied, the initially incoherent mixture can be changed to a specifically designed coherent superposition state. We also find that due to the initial conditions of the studied quantum system, the proposed methods work for different pulse orderings.

I. INTRODUCTION

Electron and hole spin states in semiconductor quantum dots (QDs) are very important in quantum information technologies.[1] Their manipulation can be efficiently achieved using optical methods, e.g., by the application of electromagnetic pulses. This has been verified, for more than a decade, by a series of important experiments for the coherent manipulation, measurement, and entanglement of individual spins in optically active quantum dots.[2,3] A particular system that has attracted significant attention in this research area is based on the spin states of a quantum dot in the Voigt geometry (see Fig. 1). Numerous novel experiments[4–17] and several theoretical proposals[18–28] have been devoted to this system.

An interesting problem for the quantum dot electron spin states in the Voigt geometry is the initialization, i.e., the preparation of one of the two electron spin states starting from an equal incoherent mixture, which is the natural initial state of the system. The main proposal for initialization involves the application of a single laser field and is based on the optical pumping process.[19] This process can be accelerated by using the Purcell effect through integration of the quantum dot structure with semiconductor microcavities,[23] photonic crystal nanocavities,[25] and plasmonic nanostructures.[26,28] Another important problem is the coherent manipulation of the electron spin states and the creation of specific superposition states or, in general, optically controlled spin rotations.[18,20–22,24,27] Starting from an incoherent mixture, specific coherent superpositions of states can be achieved by the application of two optical pulses in two-photon resonance and using the phenomenon of coherent population trapping.[1,10] The more general optically controlled spin rotations can be achieved by the application of two far-detuned optical fields in a Raman-type transition scenario[21,27] or by the application of specifically designed short pulsed fields with near resonant couplings.[18,20,24] In the latter proposal, interesting results have been obtained for hyperbolic secant electromagnetic pulses.[18,20,24]

An important method in the area of optical control of quantum systems is stimulated Raman adiabatic passage (STIRAP).[29–31] In its original scheme,[32] STIRAP uses two mutually delayed and partially overlapping laser pulses of specific time-ordering, at two-photon resonance, for the adiabatic transfer of population between the two lower states of a Λ-type quantum system. STIRAP and its basic variation, fractional STIRAP,[33–35] where the two optical pulses are initially delayed but are switched off simultaneously, have found numerous applications in the control of quantum, and many

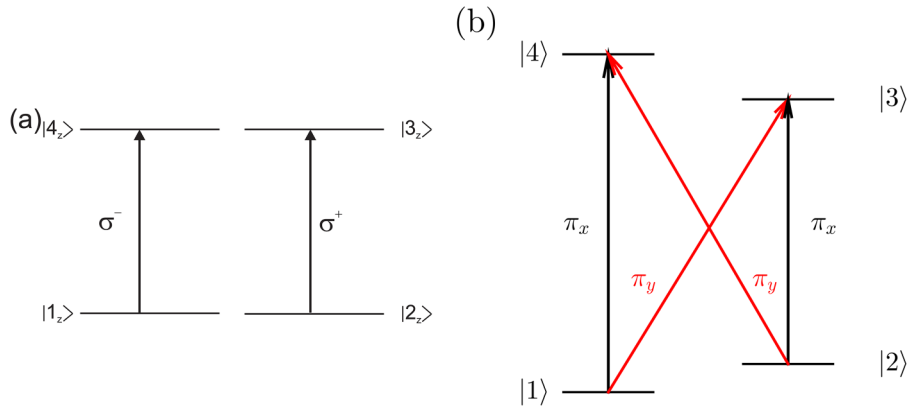

FIG. 1. (a) Four level scheme illustrating the ground and excited states of self-assembled QDs. Ground (and excited) states share the same energy. These states can be driven by circularly polarized laser fields in the absence of an external magnetic field. (b) The application of an external magnetic field perpendicular to the growth axis produces Zeeman splittings that lifts the degeneracy of ground and excited states. Transitions $|2\rangle \leftrightarrow |3\rangle$ and $|1\rangle \leftrightarrow |4\rangle$ are driven by a *x*-polarized laser field, while transitions $|1\rangle \leftrightarrow |3\rangle$ and $|2\rangle \leftrightarrow |4\rangle$ are driven by a *y*-polarized laser field.

other, structures.[30,31,36] In contrast to resonant techniques, adiabatic processes, like STIRAP, do not require specific pulse areas or pulse shapes and are robust in the weak to moderate fluctuations of the parameters of the electromagnetic fields and the quantum systems. Also, in comparison to far-detuned Raman-type transitions, which, in general, induce weak couplings and unwanted energy shifts, STIRAP induces strong couplings and works very efficiently in resonant situations, without populating the intermediate excited state, if the adiabatic conditions are met. That is why STIRAP is very useful in situations where the initial and target states interact via a lossy intermediate state. STIRAP and its many variations work with the application of the optical pulses in pure initial quantum states, and in the vast majority of studies, only one of the lower states is initially populated, as pulse ordering is rather important.[29–31]

The applications of STIRAP in semiconductor quantum dots have been analyzed in various coupling configurations, and several applications have been proposed, including manipulation of quantum states, creation of entanglement, and single-electron transfer.[22,37–46] For a positively charged quantum dot in the Voigt geometry, Sun *et al.*[22] proposed a delay-dependent non-Abelian geometric phase, which is produced by a non-adiabatic transition between two degenerate dark states. Their method works as a two step-process, with first initialization via optical pumping[19] and then applying three laser pulses in a general tripod-type configuration and using STIRAP.

In this article, we propose to use mutually delayed and partially overlapping laser pulses, similar to those used in STIRAP and fractional STIRAP, for the optical control of quantum dot spin states in the Voigt geometry. Here, the quantum dot system is taken initially in an incoherent mixture of the two electron-spin states. We show that the application of regular delayed and partially overlapping pulses, similar to those applied in original STIRAP,[32] can lead to initialization. In addition, if initially delayed, partially overlapping, and simultaneously switched off pulses are applied, similar to those applied in fractional STIRAP,[35] the initially incoherent mixture can be changed to a specifically designed coherent superposition state. The latter occurs without the prerequisite of a previous initialization. Furthermore, we find that, due to the initial conditions of the studied quantum system, the proposed methods work for different pulse orderings. The dependence of the efficiency of the proposed method on the parameters of the system is also discussed.

The article is organized as follows: In Sec. II, we describe the quantum dot system, the applied optical pulses, and the density matrix equations for the interaction of the quantum dot with the optical pulses. Then, we solve the density matrix equations numerically and present in Sec. III results for initialization and creation of coherent superposition states for several system parameters. We also offer an explanation of the behavior of the system and analyze the dependence of the proposed method on different systems' parameters. Finally, in Sec. IV, we summarize our findings.

II. THEORY

We consider a singly-charged self-assembled QD with growth direction along the *z*-axis. The ground spin states are labeled $|1_z\rangle \equiv |\downarrow_z\rangle$ and $|2_z\rangle \equiv |\uparrow_z\rangle$, while the excited trion states are $|4_z\rangle \equiv |\downarrow_z \uparrow_z \Downarrow_z\rangle$ and $|3_z\rangle \equiv |\downarrow_z \uparrow_z \Uparrow_z\rangle$. Here, $\Uparrow_z$ ($\Downarrow_z$) and $\uparrow_z$ ($\downarrow_z$) denote a heavy hole and an electron with spins along (against) the *z*-axis, respectively. The energy level diagram of such kind of QD is depicted in Fig. 1(a). The optical transition $|1_z\rangle \leftrightarrow |4_z\rangle (|2_z\rangle \leftrightarrow |3_z\rangle)$ is driven by a $\sigma^-(\sigma^+)$polarized laser field, while due to selection rules, transitions $|1_z\rangle \leftrightarrow |3_z\rangle$ and $|2_z\rangle \leftrightarrow |4_z\rangle$ remain dark.

The application of an external magnetic field along the *x*-axis, in the so-called Voigt geometry, lifts the degeneracy of

electron/hole levels. The external magnetic field also causes a reference frame transformation from the z-axis to the x-axis and we get $|2\rangle \equiv |\uparrow_x\rangle = 1/\sqrt{2}(|\uparrow_z\rangle + |\downarrow_z\rangle)$ and $|1\rangle \equiv |\downarrow_x\rangle = 1/\sqrt{2}(|\uparrow_z\rangle - |\downarrow_z\rangle)$. Now, each ground state is linked to the two excited trion states ($|4\rangle \equiv |\downarrow_x\uparrow_x\Downarrow_x\rangle$ and $|3\rangle \equiv |\downarrow_x\uparrow_x\Uparrow_x\rangle$) via linearly and orthogonally polarized transitions as depicted in Fig. 1(b). The vertical transitions ($|1\rangle \leftrightarrow |4\rangle$ and $|2\rangle \leftrightarrow |3\rangle$) can be driven with a linearly x-polarized (π_x) electromagnetic field and the diagonal transitions ($|1\rangle \leftrightarrow |3\rangle$ and $|2\rangle \leftrightarrow |4\rangle$) with a linearly y-polarized (π_y) electromagnetic field. We consider that the quantum dot interacts with two linearly polarized pulsed laser fields with orthogonal polarizations; the field with frequency ω_a (ω_b) is a π_x (π_y) field.

The Hamiltonian that describes the interaction of the optical fields with the quantum dot system, in the dipole and rotating wave approximations, is given by

$$H = \sum_{n=1}^{4} \hbar\omega_n |n\rangle\langle n| - \hbar\Big[\Omega_a(t)e^{-i\omega_a t}|4\rangle\langle 1| + \Omega_a(t)e^{-i\omega_a t}|3\rangle\langle 2| + \Omega_b(t)e^{-i\omega_b t}|3\rangle\langle 1| + \Omega_b(t)e^{-i\omega_b t}|4\rangle\langle 2| + H.c.\Big]. \tag{1}$$

Here, $\hbar\omega_n$ with $n = 1-4$ is the energy of state $|n\rangle$. Also, $\Omega_a(t)$, $\Omega_b(t)$ are the complex time-dependent Rabi frequencies defined as $\Omega_a(t) = \bar{\Omega}_a f_a(t)$, $\Omega_b(t) = \bar{\Omega}_b f_b(t)$, with $\bar{\Omega}_a = \Omega$, $\bar{\Omega}_b = \Omega e^{-i\phi}$, where ϕ is the phase difference between the two pulses, and $f_a(t)$, $f_b(t)$ are the dimensionless envelopes of the pulses with frequencies ω_a, ω_b, respectively. The Hamiltonian of Eq. (1), after a transformation, using the unitary operator $U(t) = e^{-i\sum_{n=1}^{4}\alpha_n|n\rangle\langle n|t}$, where $\alpha_1 = \omega_1$, $\alpha_2 = \omega_a - \omega_b + \omega_1$, $\alpha_3 = \omega_3 + \omega_a - \omega_{41}$, and $\alpha_4 = \omega_a + \omega_1$, gives the interaction Hamiltonian

$$\begin{aligned} H_{eff} = &-\hbar(\omega_a - \omega_b - \omega_{21})|2\rangle\langle 2| - \hbar(\omega_a - \omega_{41})|3\rangle\langle 3| \\ &- \hbar(\omega_a - \omega_{41})|4\rangle\langle 4| - \hbar\Big[\Omega_a(t)|4\rangle\langle 1| \\ &+ \Omega_b(t)|4\rangle\langle 2| + \Omega_a(t)e^{-i(\omega_a-\omega_b+\omega_{43})t}|3\rangle\langle 2| \\ &+ \Omega_b(t)e^{i(\omega_a-\omega_b-\omega_{43})t}|3\rangle\langle 1| + H.c.\Big], \end{aligned} \tag{2}$$

with $\omega_{nm} = \omega_n - \omega_m$. Also, ω_{21} (ω_{43}) is the Zeeman splitting of the single-electron spin states (heavy-hole spin trion states). Using the Hamiltonian of Eq. (2), we obtain the equations for the density matrix elements of the system. The explicit form of the equations is shown in the Appendix.

We will assume that the two laser pulses are at two-photon resonance, $\omega_a - \omega_b = \omega_{21}$. The dimensionless pulse envelopes are taken as

$$f_a(t) = \sin(\theta)e^{-(t-t_0-\eta/2)^2/(2t_p^2)}, \tag{3}$$

$$f_b(t) = \cos(\theta)e^{-(t-t_0-\eta/2)^2/(2t_p^2)} + e^{-(t-t_0+\eta/2)^2/(2t_p^2)}, \tag{4}$$

where η is the pulse delay, t_0 determines the center of the laser pulses for $\eta = 0$, t_p determines the width of the pulses, and $0 \le \theta \le \pi/2$. For $\theta = \pi/2$,

$$f_a(t) = e^{-(t-t_0-\eta/2)^2/(2t_p^2)}, \quad f_b(t) = e^{-(t-t_0+\eta/2)^2/(2t_p^2)}, \tag{5}$$

so the pulses become regular Gaussian-shape, and for $\eta \neq 0$ are applied with a time delay between them. For $\theta \neq \pi/2$ and $\eta > 0$, the laser pulses switch on with a respective initial delay, but they switch off simultaneously. The latter coupling can also be realized with interrupted laser pulses,[33–35] but the above choice of Eqs. (3) and (4) gives a smooth realization of the required evolution.[35] We note that the present idea is not limited to the above pulses; it may be realized with several other pulse shapes as well.[29,30,35,47]

III. NUMERICAL RESULTS

In Figs. 2–6, we present calculations for the evolution of the population of the four quantum states for different cases of the applied optical fields. We assume that the excited trion states decay to the ground spin states with the same population decay rate Γ. For these figures, and for the rest of the article, unless stated otherwise, the parameters of the quantum dot are taken as $\hbar\Gamma = 1.2\,\mu$eV, $\hbar\omega_{21} = 0.124$ meV, $\hbar\omega_{43} = 0.078$ meV (the Zeeman splittings correspond to magnetic field ~8 T), typical for InAs quantum dots.[19,20] The laser with frequency ω_a is taken at exact resonance with the transition $|1\rangle \leftrightarrow |4\rangle$, e.g., $\omega_a = \omega_{41}$, and the laser with frequency ω_b is taken at exact resonance with the transition $|2\rangle \leftrightarrow |4\rangle$, e.g., $\omega_b = \omega_{42}$. The parameters for the laser fields are taken as $\Omega = 10\ \text{ns}^{-1}$, $t_p = 1.5$ ns, $t_0 = 5t_p$, unless stated otherwise. In all the calculations in this article, the quantum dot system is in an initial incoherent mixture of the two electron-spin states, $\rho_{11}(0) = 1/2$, $\rho_{22}(0) = 1/2$, $\rho_{33}(0) = \rho_{44}(0) = 0$, and $\rho_{nm}(0) = 0$ with $n \neq m$.

In Fig. 2, we present the time evolution of the population in the different states for the system interacting with Gaussian pulses of Eq. (5) and the corresponding pulse envelopes. In the first (second) case, the pulse with frequency ω_b (ω_a) precedes that with frequency ω_a (ω_b) in both switch on and switch off [see Figs. 2(a) and 2(b)]. The dynamics of the population in Fig. 2(c), which corresponds to the first case, shows that the population is partially transferred for short times to state $|1\rangle$, but at later times, it is efficiently, almost completely, transferred to state $|2\rangle$. Also, in the early part of the evolution, state $|4\rangle$ has some transient population; however, at later times, its population remains negligible. A qualitatively similar behavior is obtained in the second case, shown in Fig. 2(d), but now the population is partially transferred for early times to state $|2\rangle$, and at later times, it is efficiently, almost completely, transferred to state $|1\rangle$. With this method, the initialization of either state $|1\rangle$ or $|2\rangle$ can be achieved.

Then, in Fig. 3, we present the time evolution of the population in the different states for the system interacting with pulses with their envelope described by Eqs. (3) and (4) and the corresponding pulse envelopes. In the first (second) case, the pulse with frequency ω_b (ω_a) precedes that with frequency ω_a (ω_b) at early times and then both pulses switch off together

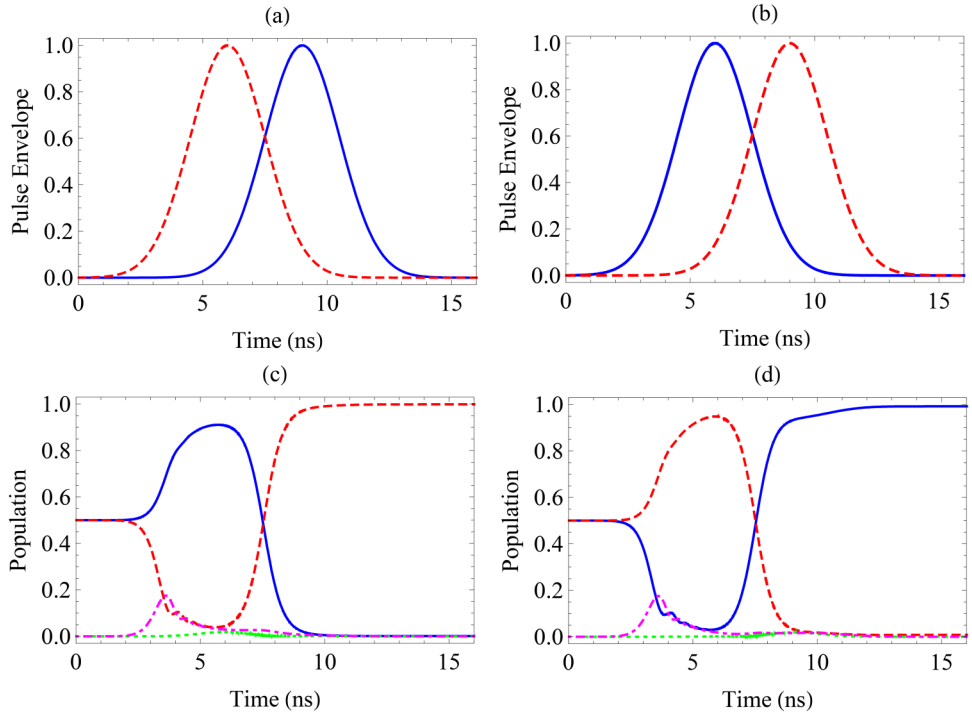

FIG. 2. The pulse envelope, (a) and (b), and the time evolution, (c) and (d), of the population, $\rho_{nn}(t)$ with $n = 1 - 4$, of states $|1\rangle$ (solid curve), $|2\rangle$ (dashed curve), $|3\rangle$ (dotted curve), and $|4\rangle$ (dash-dotted curve) for Gaussian pulses of Eq. (5) with $\eta = 3$ ns for (a) and (c) and $\eta = -3$ ns for (b) and (d).

[see Figs. 3(a) and 3(b)]. In order to achieve this, for Figs. 3(a) and 3(c), we use the envelopes described by Eqs. (3) and (4), while for Figs. 3(b) and 3(d), we use the form of $f_a(t)$ for $f_b(t)$ and vice versa. In both cases, $\theta = \pi/4$ and $\phi = 0$. The dynamics of the population in Fig. 3(c) shows a partial population transfer for short times to state $|1\rangle$, but at later times, the population is equally divided between states $|1\rangle$ and $|2\rangle$. Also, in the early part of the evolution, state $|4\rangle$ has some transient population; however, at later times, its population remains very small. A qualitatively similar behavior is obtained in Fig. 3(d), with the difference that the population is partially transferred for early times to state $|2\rangle$, but at later times, in this case too, the population is equally divided between states $|1\rangle$ and $|2\rangle$. Although, in both cases, the population is initially and finally equally divided between states $|1\rangle$ and $|2\rangle$, the initial and final states are completely different, and this can be seen in Fig. 4, where the time evolution of the coherence $\rho_{12}(t)$ is presented. It is clear that initially we have a mixed state, while finally, a coherent superposition of the form $(|1\rangle - |2\rangle)/\sqrt{2}$ is formed.

The creation of a coherent superposition is also explored in Figs. 5 and 6. Figure 5 presents results for the same parameters as in Fig. 3(a) but with $\phi = \pi$. The evolution of the population is found to be the same as in Fig. 3(c), but in this case, a coherent superposition of the form $(|1\rangle + |2\rangle)/\sqrt{2}$ is created. Also, in Fig. 6, we present results for the pulse envelopes and the time evolution of the population of all states and the coherence $\rho_{12}(t)$ for the same parameters as in Fig. 3(a) but with $\theta = \pi/3$. The dynamics of the population in Fig. 6(b) shows a partial population transfer for short times to state $|1\rangle$, but in later times, the population in state $|1\rangle$ becomes almost 1/4 and in state $|2\rangle$, 3/4. In addition, Fig. 6(c) shows the creation of a coherent superposition of the form $(|1\rangle - \sqrt{3}|2\rangle)/2$. Interestingly, although the form of the applied pulses is similar to those applied in the STIRAP method[29–32] or in its variation fractional STIRAP[33–35] in the studied problem, as the numerical results reveal, since the initial condition is an equal incoherent mixture, the initialization or the creation of a specific superposition state can be created in both pulse orderings, i.e., when pulse with frequency ω_a (ω_b) precedes that of ω_b (ω_a).

We will now present an explanation of the behavior of the system. As the two pulses are applied at two-photon resonance $\omega_a = \omega_b + \omega_{21}$ and $\omega_{21} \pm \omega_{43} > \Omega$, we can assume that the terms with $e^{\pm i(\omega_a - \omega_b \pm \omega_{43})t}$ can be omitted from the Hamiltonian of Eq. (2), so effectively, we get a three-level Λ-type system for states $|1\rangle$, $|2\rangle$, and $|4\rangle$, while state $|3\rangle$ is essentially decoupled. The effective Hamiltonian for this reduced system is

$$H_\Lambda = -\hbar(\omega_a - \omega_{41})|3\rangle\langle 3| - \hbar(\omega_a - \omega_{41})|4\rangle\langle 4| - \hbar\Big[\Omega f_a(t)|4\rangle\langle 1| + \Omega e^{i\phi} f_b(t)|4\rangle\langle 2| + \text{H.c.}\Big]. \quad (6)$$

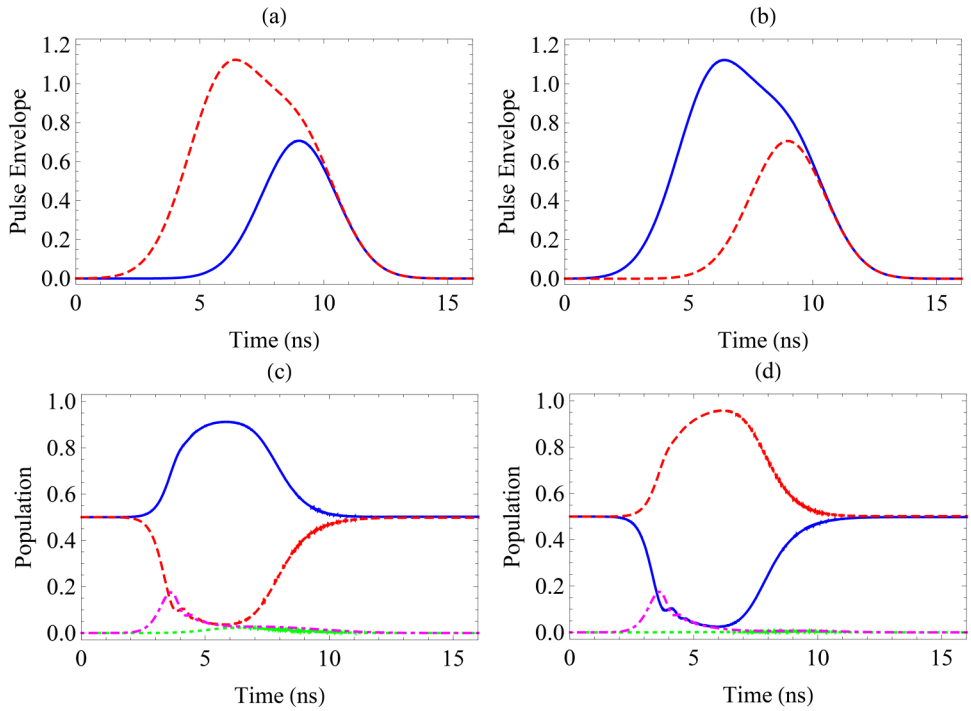

FIG. 3. The pulse envelope, (a), and the time evolution, (c), of the population of states $|1\rangle$ (solid curve), $|2\rangle$ (dashed curve), $|3\rangle$ (dotted curve), and $|4\rangle$ (dash-dotted curve) for pulses with envelope given by Eqs. (3) and (4) with $\eta = 3$ ns, $\theta = \pi/4$, and $\phi = 0$. In (b) and (d), we present the same results but interchanging the form of the pulse envelopes.

This Hamiltonian under the application of delayed laser pulses is the same as the one used for the description of STIRAP and has been studied in detail.[29–31,35] An important issue is the existence of an eigenstate with a zero eigenvalue, the so-called dark state, which has the form, up to an overall phase,

$$|\psi_{dark}(t)\rangle = \frac{f_b(t)}{\sqrt{f_a^2(t)+f_b^2(t)}}|1\rangle - e^{i\phi}\frac{f_a(t)}{\sqrt{f_a^2(t)+f_b^2(t)}}|2\rangle. \quad (7)$$

The evolution of the quantum dot spin presented above is understood if we split the dynamics into two parts. In the studied case, the population is initially divided between the two lower states $|1\rangle$ and $|2\rangle$ and the system has no initial coherence. At early times, only one laser pulse is applied. Then, at this time period, the non-driven lower state, state $|2\rangle$ ($|1\rangle$) if the laser with frequency ω_a (ω_b) is applied first, gains population via optical pumping.[19] Then, after the second field is switched on, the system can be described by the Hamiltonian of Eq. (6) and, if the interaction is adiabatic, the system follows the evolution of the dark state, Eq. (7). In that part, if $\theta = \pi/2$, the population can be completely transferred to state $|1\rangle$ ($|2\rangle$) if the laser with frequency ω_a (ω_b) is switched off prior to the laser with frequency ω_b (ω_a). Also, for $\theta \neq \pi/2$ and $\eta > 0$, the adiabatic following of the dark state, Eq. (7), leads to the superposition state at the end of the pulses, i.e., for $t = t_f$:

$$|\psi_{dark}(t_f)\rangle = \cos(\theta)|1\rangle - e^{i\phi}\sin(\theta)|2\rangle, \quad (8)$$

so, $\rho_{11}(t_f) = \cos^2(\theta)$, $\rho_{22}(t_f) = \sin^2(\theta)$, $\rho_{12}(t_f) = -e^{-i\phi}\cos(\theta)\sin(\theta)$. Therefore, starting from an incoherent mixture of the two electron-spin states, depending on the evolution of the applied laser fields, either initialization of a specific electron-spin state or a general coherent superposition of the two electron-spin states can be created. The later part of the dynamics, i.e., after the second field is switched on, is similar to that of STIRAP or fractional STIRAP, depending on the form of the pulses.

The above analysis can be used for determining the parameters of the applied pulses which can be used for the successful implementation of the described procedure. In order to achieve efficient adiabatic evolution of the system, Ωt_p should be, typically, larger than 15 and $\eta > t_p$.[31] In addition, for having efficient transfer in the early part of the evolution, t_p should be larger than $1/\Gamma$. The efficiency of the proposed method is shown in Fig. 7, where we calculate the fidelity $F(|\psi\rangle, \rho) = \sqrt{\langle\psi|\rho|\psi\rangle}$ for creating a target state $|\psi\rangle$ as a function of the parameters of the applied fields (maximum Rabi frequency, pulse width, and pulse delay). Here, $|\psi\rangle$ is a pure state and ρ is the density matrix of the system.[48] We consider the preparation of state $|2\rangle$ and the preparation of

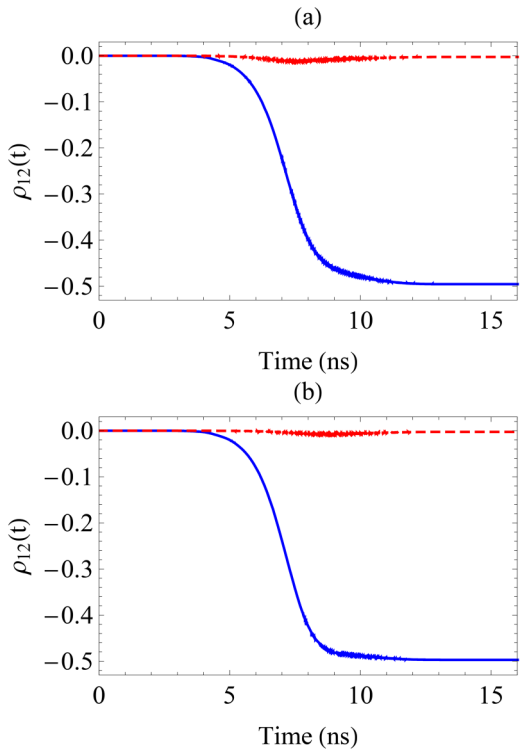

FIG. 4. Time evolution of the real (solid curve) and imaginary (dotted curve) parts of the quantum coherence term $\rho_{12}(t)$ for the same parameters as in Fig. 3. Panel (a) corresponds to Fig. 3(a) and panel (b) to Fig. 3(b).

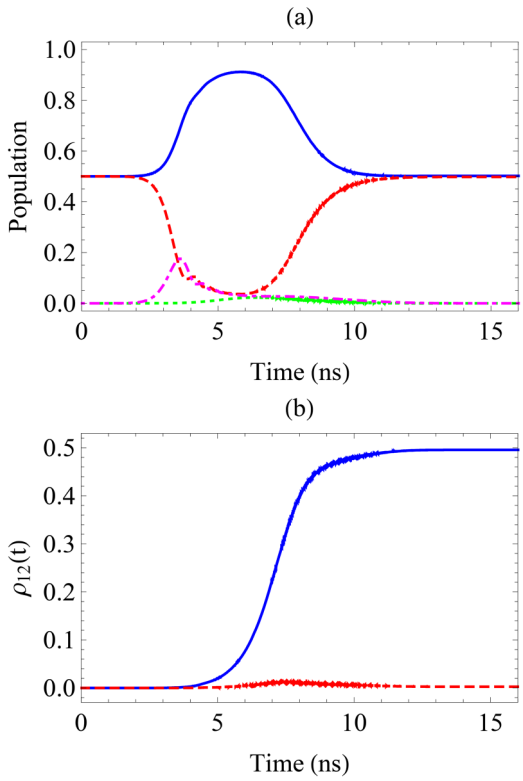

FIG. 5. Time evolution of (a) the population of states $|1\rangle$ (solid curve), $|2\rangle$ (dashed curve), $|3\rangle$ (dotted curve), and $|4\rangle$ (dash-dotted curve) and (b) the real (solid curve) and imaginary (dotted curve) parts of the quantum coherence term $\rho_{12}(t)$ for pulses with envelope given by Eqs. (3) and (4) with $\eta = 3$ ns, $\theta = \pi/4$, and $\phi = \pi$.

the superposition state $(|1\rangle - |2\rangle)/\sqrt{2}$ using the methodology presented above. We also present the results for a single Gaussian pulse that creates state $|2\rangle$ via optical pumping[19] and two Gaussian pulses at two-photon resonance that prepare the superposition state $(|1\rangle - |2\rangle)/\sqrt{2}$ via coherent population trapping. We find that the proposed method gives high fidelities for preparation of both a single state or a coherent superposition state which are comparable to and in several cases higher than optical pumping or coherent population trapping. Our findings verify that the proposed method works with high efficiency for delayed but overlapping, strong and relatively long, electromagnetic pulses. However, due to its adiabatic nature, the method does not require specific values of these parameters and works properly for a wide range of pulse delays, laser intensities, and pulse lengths. Finally, for these parameters, the initialization process of a specific state is found to be more robust than the creation of the coherent superposition process. We note that STIRAP is also more robust than fractional STIRAP.[31,35] The fidelities can become even higher if one uses optimized applied pulses,[47] instead of the simple pulses that we used here.

We will also comment on the effective duration of the preparation process. As the dynamics of the system is adiabatic, an exact transition time cannot be determined. A good estimate for the transition time for creating a single state is the time it takes for the population of the target state to rise from ε to $1-\varepsilon$, where $0 < \varepsilon \ll 1$. For Gaussian pulses, this leads to[31,49]

$$T = \frac{2t_p^2}{\eta}\ln\left(\frac{1}{\varepsilon} - 1\right). \tag{9}$$

This time turns out to be about twice the one needed for the optical pumping approach.

We also explore the dependence of our proposed scheme on the decay rate Γ for the typical range of decay rates appearing in the quantum dots of interest. In Fig. 8, we present the fidelity as a function of the decay rate Γ for the preparation of state $|2\rangle$ and the preparation of the superposition state $(|1\rangle - |2\rangle)/\sqrt{2}$. We also present the results for a single Gaussian pulse that creates state $|2\rangle$ via optical pumping,[19] as well as the fidelity of the creation of the superposition state $(|1\rangle - |2\rangle)/\sqrt{2}$ using coherent population trapping by the application of two pulses in two-photon resonance. The figure indicates that efficient initialization and creation of a superposition state can be

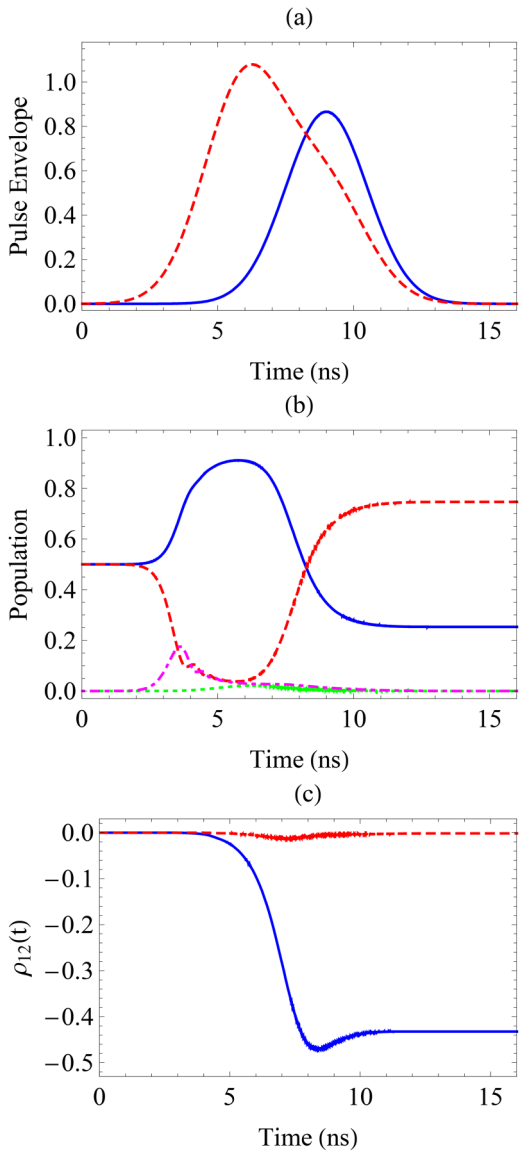

FIG. 6. The pulse envelope, (a), and the time evolution of (b) the population of states $|1\rangle$ (solid curve), $|2\rangle$ (dashed curve), $|3\rangle$ (dotted curve), and $|4\rangle$ (dash-dotted curve) and (c) the real (solid curve) and imaginary (dotted curve) parts of the quantum coherence term $\rho_{12}(t)$ for pulses with envelope given by Eqs. (3) and (4) with $\eta = 3$ ns, $\theta = \pi/3$, and $\phi = 0$.

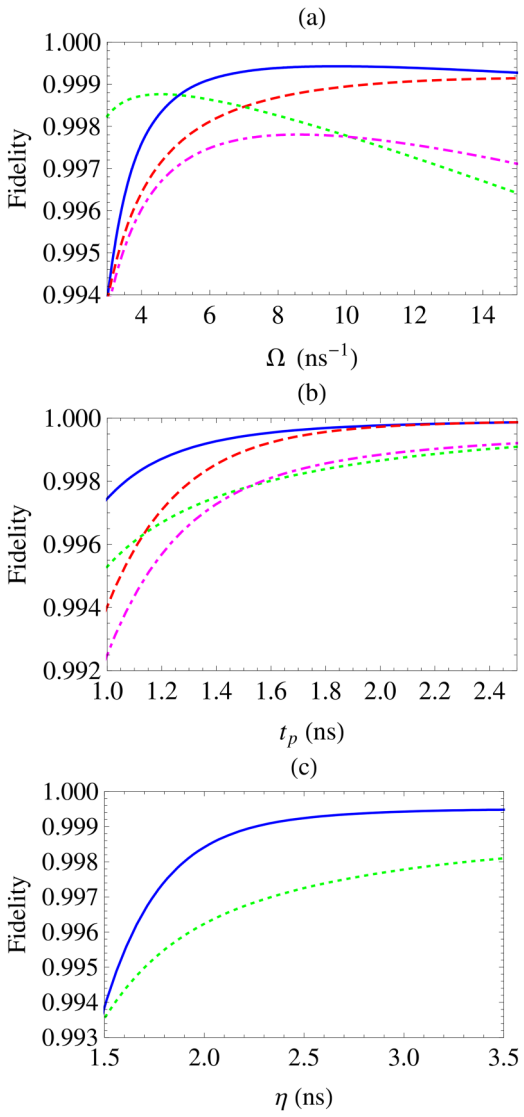

FIG. 7. (a) Fidelity as a function of the maximum Rabi frequency Ω for two Gaussian pulses of Eq. (5) (solid curve), for a single pulse $f_a(t) = e^{-(t-t_0-\eta/2)^2/(2t_p^2)}$, $f_b(t) = 0$ (dashed curve), for pulses with envelope given by Eqs. (3) and (4) with $\theta = \pi/4$ and $\phi = 0$ (dotted curve), and for pulses given by $f_a(t) = \sin(\theta)e^{-(t-t_0-\eta/2)^2/(2t_p^2)}$, $f_b(t) = \cos(\theta)e^{-(t-t_0-\eta/2)^2/(2t_p^2)}$, with $\theta = \pi/4$ and $\phi = 0$ (dot-dashed curve). (b) Fidelity as a function of t_p for the same cases as (a). (c) Fidelity as a function of the delay between the two pulses η for two Gaussian pulses of Eq. (5) (solid curve) and for pulses with envelope given by Eqs. (3) and (4) with $\theta = \pi/4$ and $\phi = 0$ (dotted curve). In all the cases, the results are presented for $t_f = 2t_0 + \eta$.

achieved using the proposed method for almost all the range of values of the decay rate. Here, again, the initialization process is more robust to the change of Γ than the creation of the coherent superposition process. There is a small reduction of the efficiency of the process for large decay rates, as the increase of Γ above certain values influences the evolution of the quantum dot states with incoherent population redistribution via decay. Also, we note that the fidelity of the process for small decay rates can be enhanced by increasing the pulse duration. The achieved fidelities with the proposed method are comparable, and in certain cases higher, than when using optical pumping or coherent population trapping.

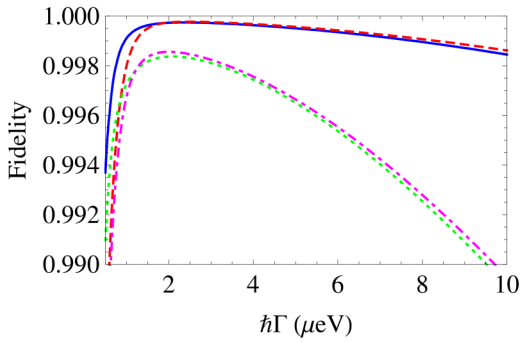

FIG. 8. Fidelity as a function of the decay rate Γ for two Gaussian pulses of Eq. (5) (solid curve), for a single pulse $f_a(t) = e^{-(t-t_0-\eta/2)^2/(2t_p^2)}$, $f_b(t) = 0$ (dashed curve), for pulses with envelope given by Eqs. (3) and (4) with $\theta = \pi/4$ and $\phi = 0$ (dotted curve), and for pulses given by $f_a(t) = \sin(\theta)e^{-(t-t_0-\eta/2)^2/(2t_p^2)}$, $f_b(t) = \cos(\theta)e^{-(t-t_0-\eta/2)^2/(2t_p^2)}$, with $\theta = \pi/4$ and $\phi = 0$ (dot-dashed curve). The calculations are for $\eta = 3$ ns. The results are presented for $t_f = 2t_0 + \eta$.

IV. SUMMARY

In this work, we used mutually delayed and partially overlapping laser pulses, similar to those used in STIRAP and fractional STIRAP, for the optical control of quantum dot spin states in the Voigt geometry. We considered the case that the quantum dot system is initially in an incoherent mixture of the two electron-spin states, which is the natural initial state of the studied quantum dot system. We showed that the application of regular delayed and partially overlapping pulses can lead to initialization. In addition, the application of initially delayed, partially overlapping, and simultaneously switched off pulses changes the initial incoherent mixture to a specifically designed coherent superposition state. The latter occurs without the prerequisite of a previous initialization. Furthermore, we found that, due to the initial conditions of the studied quantum system, the proposed methods work for different pulse orderings. A simplified model that explains the results was also presented. The proposed method was found to be robust against changes to the parameters of the quantum dot and the applied optical fields, such as the decay rate and pulse delay, intensity, and pulse width. We believe that the proposed method may find interesting applications in optically controlled quantum dot spin states for quantum information processing.

ACKNOWLEDGMENTS

E.P. acknowledges useful discussions with Dr. Dionisis Stefanatos. F.C. acknowledges the support of UCM-Banco de Santander Research Project No. PR41/17-21033, support of MICINN through Project No. FIS2017-87360-P, and funding to MECD through Grant No. PRX16/00473. E.P. acknowledges support through the Operational Program "Human Resources Development, Education and Lifelong Learning" which is co-financed by the European Union (EU) (European Social Fund) and Greek national funds. S.E.E. acknowledges support from the National Science Foundation (award number 1839056).

APPENDIX: DENSITY MATRIX EQUATIONS

The density matrix equations of the system are given by

$$\dot{\rho}_{11}(t) = \gamma_{41}\rho_{44}(t) + \gamma_{31}\rho_{33}(t) + i\Omega_a^*(t)\rho_{41}(t) - i\Omega_a(t)\rho_{14}(t) + i\Omega_b^*(t)\rho_{31}(t)e^{-i(\omega_a-\omega_b-\omega_{43})t} - i\Omega_b(t)\rho_{13}(t)e^{i(\omega_a-\omega_b-\omega_{43})t}, \tag{A1}$$

$$\dot{\rho}_{22}(t) = \gamma_{32}\rho_{33}(t) + \gamma_{42}\rho_{44}(t) + i\Omega_a^*(t)\rho_{32}(t)e^{i(\omega_a-\omega_b+\omega_{43})t} - i\Omega_a(t)\rho_{23}(t)e^{-i(\omega_a-\omega_b+\omega_{43})t} + i\Omega_b^*(t)\rho_{42}(t) - i\Omega_b(t)\rho_{24}(t), \tag{A2}$$

$$\dot{\rho}_{33}(t) = -(\gamma_{31}+\gamma_{32})\rho_{33}(t) + i\Omega_a(t)\rho_{23}(t)e^{-i(\omega_a-\omega_b+\omega_{43})t} - i\Omega_a^*(t)\rho_{32}(t)e^{i(\omega_a-\omega_b+\omega_{43})t} + i\Omega_b(t)\rho_{13}(t)e^{i(\omega_a-\omega_b-\omega_{43})t} - i\Omega_b^*(t)\rho_{31}(t)e^{-i(\omega_a-\omega_b-\omega_{43})t}, \tag{A3}$$

$$\dot{\rho}_{44}(t) = -(\gamma_{41}+\gamma_{42})\rho_{44}(t) + i\Omega_a(t)\rho_{14}(t) - i\Omega_a^*(t)\rho_{41}(t) + i\Omega_b(t)\rho_{24}(t) - i\Omega_b^*(t)\rho_{42}(t), \tag{A4}$$

$$\dot{\rho}_{14}(t) = -[i(\omega_a-\omega_{41})+\Gamma_{14}]\rho_{14}(t) + i\Omega_a^*(t)[\rho_{44}(t)-\rho_{11}(t)] + i\Omega_b^*(t)\rho_{34}(t)e^{-i(\omega_a-\omega_b-\omega_{43})t} - i\Omega_b^*(t)\rho_{12}(t), \tag{A5}$$

$$\dot{\rho}_{13}(t) = -[i(\omega_a-\omega_{41})+\Gamma_{13}]\rho_{13}(t) + i\Omega_b^*(t)[\rho_{33}(t)-\rho_{11}(t)]e^{-i(\omega_a-\omega_b-\omega_{43})t} + i\Omega_a^*(t)\rho_{43}(t) - i\Omega_a^*(t)\rho_{12}(t)e^{i(\omega_a-\omega_b+\omega_{43})t}, \tag{A6}$$

$$\dot{\rho}_{12}(t) = -[i(\omega_a-\omega_b-\omega_{21})+\Gamma_{12}]\rho_{12}(t) + i\Omega_a^*(t)\rho_{42}(t) + i\Omega_b^*(t)\rho_{32}(t)e^{-i(\omega_a-\omega_b-\omega_{43})t} - i\Omega_a^*(t)\rho_{13}(t)e^{-i(\omega_a-\omega_b+\omega_{43})t} - i\Omega_b(t)\rho_{14}(t), \tag{A7}$$

$$\dot{\rho}_{34}(t) = -\Gamma_{34}\rho_{34}(t) + i\Omega_a(t)\rho_{24}(t)e^{-i(\omega_a-\omega_b+\omega_{43})t} + i\Omega_b(t)\rho_{14}(t)e^{i(\omega_a-\omega_b-\omega_{43})t} - i\Omega_a^*(t)\rho_{31}(t) - i\Omega_b^*(t)\rho_{32}(t), \tag{A8}$$

$$\dot{\rho}_{24}(t) = -[i(\omega_b-\omega_{42})+\Gamma_{24}]\rho_{24}(t) + i\Omega_a^*(t)\rho_{34}(t)e^{i(\omega_a-\omega_b+\omega_{43})t} + i\Omega_b^*(t)[\rho_{44}(t)-\rho_{22}(t)] - i\Omega_a^*(t)\rho_{21}(t), \tag{A9}$$

$$\dot{\rho}_{23}(t) = -[i(\omega_b-\omega_{42})+\Gamma_{23}]\rho_{23}(t) + i\Omega_a^*(t)[\rho_{33}(t)-\rho_{22}(t)]e^{i(\omega_a-\omega_b+\omega_{43})t} + i\Omega_b^*(t)\rho_{43}(t) - i\Omega_b^*(t)\rho_{21}(t)e^{-i(\omega_a-\omega_b-\omega_{43})t}, \tag{A10}$$

with $\rho_{nm}(t) = \rho_{mn}^*(t)$. Here, γ_{nm} are the population decay rates and $\Gamma_{nm} = \Gamma_{mn}$ the coherence decay rates, which are given by $\Gamma_{14} = \Gamma_{24} = (\gamma_{41}+\gamma_{42})/2$, $\Gamma_{13} = \Gamma_{23} = (\gamma_{31}+\gamma_{32})/2$, $\Gamma_{34} = (\gamma_{31}+\gamma_{32}+\gamma_{41}+\gamma_{42})/2$, and $\Gamma_{12} = 0$. For simplicity, and in accordance to

previous work,[19–21,23,25,26,28] we take $\gamma_{31} = \gamma_{32} = \gamma_{41} = \gamma_{42} = \Gamma$. We note that in Eq. (A1), there should be a spontaneously generated coherence term[50], which in the limit of the magnetic field being zero gives the circularly polarized selection rules. However, in the limit of large Zeeman splitting compared to the decay rate, that we use here, this term is safely omitted.

REFERENCES

[1]R.-B. Liu, W. Yao, and L. J. Sham, Adv. Phys. **59**, 703 (2010).
[2]R. J. Warburton, Nat. Mater. **12**, 483 (2013).
[3]W. B. Gao, A. Imamoglu, H. Bernien, and R. Hanson, Nat. Photonics **9**, 363 (2015).
[4]R. J. Warburton, C. Schäflein, D. Haft, F. Bickel, A. Lorke, K. Karrai, J. M. García, W. Schoenfeld, and P. M. Petroff, Nature **405**, 926 (2000).
[5]M. Atatüre, J. Dreiser, A. Badolato, A. Högele, K. Karrai, and A. Imamoglu, Science **312**, 551 (2006).
[6]X. Xu, Y. Wu, B. Sun, Q. Huang, J. Cheng, D. G. Steel, A. S. Bracker, D. Gammon, C. Emary, and L. J. Sham, Phys. Rev. Lett. **99**, 097401 (2007).
[7]Y. Wu, E. D. Kim, X. Xu, J. Cheng, D. G. Steel, A. S. Bracker, D. Gammon, S. E. Economou, and L. J. Sham, Phys. Rev. Lett. **99**, 097402 (2007).
[8]A. J. Ramsay, S. J. Boyle, R. S. Kolodka, J. B. B. Oliveira, J. Skiba-Szymanska, H. Y. Liu, M. Hopkinson, A. M. Fox, and M. S. Skolnick, Phys. Rev. Lett. **100**, 197401 (2008).
[9]D. Press, T. D. Ladd, B. Zhang, and Y. Yamamoto, Nature **456**, 218 (2008).
[10]X. Xu, B. Sun, P. R. Berman, D. G. Steel, A. S. Bracker, D. Gammon, and L. J. Sham, Nat. Phys. **4**, 692 (2008).
[11]M. Kroner, K. M. Weiss, B. Biedermann, S. Seidl, A. W. Holleitner, A. Badolato, P. M. Petroff, P. Öhberg, R. J. Warburton, and K. Karrai, Phys. Rev. B **78**, 075429 (2008).
[12]A. Greilich, S. E. Economou, S. Spatzek, D. R. Yakovlev, D. Reuter, A. D. Wieck, T. L. Reinecke, and M. Bayer, Nat. Phys. **5**, 262 (2009).
[13]D. Brunner, B. D. Gerardot, P. A. Dalgarno, G. Wóst, K. Karrai, N. G. Stoltz, P. M. Petroff, and R. J. Warburton, Science **325**, 70 (2009).
[14]K. De Greve, P. L. McMahon, D. Press, T. D. Ladd, D. Bisping, C. Schneider, M. Kamp, L. Worschech, S. Hofling, A. Forchel, and Y. Yamamoto, Nat. Phys. **7**, 872 (2011).
[15]L. Yu *et al.*, Nat. Commun. **6**, 8955 (2015).
[16]A. Delteil, Z. Sun, W.-B. Gao, E. Togan, S. Faelt, and A. Imamoglu, Nat. Phys. **12**, 218 (2016).
[17]J. P. Lee, A. J. Bennett, R. M. Stevenson, D. J. P. Ellis, I. Farrer, D. A. Ritchie, and A. J. Shields, Quantum Sci. Technol. **3**, 024008 (2018).
[18]S. E. Economou, L. J. Sham, Y. Wu, and D. G. Steel, Phys. Rev. B **74**, 205415 (2006).
[19]C. Emary, X. Xu, D. G. Steel, S. Saikin, and L. J. Sham, Phys. Rev. Lett. **98**, 047401 (2007).
[20]S. E. Economou and T. L. Reinecke, Phys. Rev. Lett. **99**, 217401 (2007).
[21]C. Emary and L. J. Sham, J. Phys. Condens. Matter **19**, 056203 (2007).
[22]H. Sun, X.-L. Feng, C. Wu, J.-M. Liu, S.-Q. Gong, and C. H. Oh, Phys. Rev. B **80**, 235404 (2009).
[23]V. Loo, L. Lanco, O. Krebs, P. Senellart, and P. Voisin, Phys. Rev. B **83**, 033301 (2011).
[24]S. E. Economou, Phys. Rev. B **85**, 241401(R) (2012).
[25]A. Majumdar, P. Kaer, M. Bajcsy, E. D. Kim, K. G. Lagoudakis, A. Rundquist, and J. Vuckovic, Phys. Rev. Lett. **111**, 027402 (2013).
[26]M. A. Antón, F. Carreño, S. Melle, O. G. Calderón, E. Cabrera-Granado, and M. R. Singh, Phys. Rev. B **87**, 195303 (2013).
[27]J. Hildmann and G. Burkard, Phys. Status Solidi B **251**, 1938 (2014).
[28]F. Carreño, F. Arrieta-Yáñez, and M. A. Antón, Opt. Commun. **343**, 97 (2015).
[29]K. Bergmann, H. Theuer, and B. W. Shore, Rev. Mod. Phys. **70**, 1003 (1998).
[30]P. Kral, I. Thanopulos, and M. Shapiro, Rev. Mod. Phys. **79**, 53 (2007).
[31]N. V. Vitanov, A. A. Rangelov, B. W. Shore, and K. Bergmann, Rev. Mod. Phys. **89**, 015006 (2017).
[32]J. R. Kuklinski, U. Gaubatz, F. T. Hioe, and K. Bergmann, Phys. Rev. A **40**, 6741 (1989).
[33]P. Marte, P. Zoller, and J. L. Hall, Phys. Rev. A **44**, R4118 (1991).
[34]M. Weitz, B. C. Young, and S. Chu, Phys. Rev. Lett. **73**, 2563 (1994).
[35]N. V. Vitanov, K.-A. Suominen, and B. W. Shore, J. Phys. B **32**, 4535 (1999).
[36]R. Menchon-Enrich, A. Benseny, V. Ahufinger, A. D. Greentree, Th. Busch, and J. Mompart, Rep. Prog. Phys. **79**, 074401 (2016).
[37]U. Hohenester, F. Troiani, E. Molinari, G. Panzarini, and C. Machiavello, Appl. Phys. Lett. **77**, 1864 (2000).
[38]E. Pazy, I. D'Amico, P. Zanardi, and F. Rossi, Phys. Rev. B **64**, 195320 (2001).
[39]T. Brandes, F. Renzoni, and R. H. Blick, Phys. Rev. B **64**, 035319 (2001).
[40]F. Troiani, E. Molinari, and U. Hohenester, Phys. Rev. Lett. **90**, 206802 (2003).
[41]P. Chen, C. Piermarocchi, L. J. Sham, D. Gammon, and D. G. Steel, Phys. Rev. B **69**, 075320 (2004).
[42]K. Roszak, A. Grodecka, P. Machnikowski, and T. Kuhn, Phys. Rev. B **71**, 195333 (2005).
[43]J. Fabian and U. Hohenester, Phys. Rev. B **72**, 201304(R) (2005).
[44]U. Hohenester, J. Fabian, and F. Troiani, Opt. Commun. **264**, 426 (2006).
[45]T. S. Koh, S. N. Coppersmith, and M. Friesen, Proc. Natl. Acad. Sci. U.S.A. **110**, 19695 (2013).
[46]A. Fountoulakis and E. Paspalakis, J. Appl. Phys. **113**, 174301 (2013).
[47]G. S. Vasilev, A. Kuhn, and N. V. Vitanov, Phys. Rev. A **80**, 013417 (2009).
[48]M. A. Nielsen and I. L. Chuang, *Quantum Computation and Quantum Information* (Cambridge University Press, Cambridge, 2000), sect. 9.2.2.
[49]I. I. Boradjiev and N. V. Vitanov, Phys. Rev. A **82**, 043407 (2010).
[50]S. E. Economou, R.-B. Liu, L. J. Sham, and D. G. Steel, Phys. Rev. B **71**, 195327 (2005).